Available online at www.sciencedirect.com
SCIENCE DIRECT
Journal of Magnetic Resonance 181 (2006) 262–270
JMR Journal of Magnetic Resonance
www.elsevier.com/locate/jmr

Fixed lock-time relaxation dispersion in the rotating frame

Josefina Perlo, Esteban Anoardo *

Facultad de Matemática, Astronomía y Física, Universidad Nacional de Córdoba and CONICET, X5016LAE Córdoba, Argentina

Received 8 March 2006; revised 9 May 2006
Available online 9 June 2006

Abstract

The spin-lattice relaxation dispersion may be probed in the laboratory frame through field-cycling NMR relaxometry. The experiment, as usually done, has the basic weakness that the low frequency end of the measured dispersion can be blurred by the presence of local fields. An understanding of the nature of such local fields was found to be essential to the interpretation of the dispersion profile. In this work, an attempt was made to determine the extent to which specific information can be obtained from a rotating frame experiment. The technique consists in the study of the NMR signal dispersion at a fixed spin-lock time, as a function of the radio frequency field intensity. Within this scheme, a strong dispersion can be attributed to the presence of a non-zero magnetic field component along the laboratory-frame Zeeman-axis in the rotating-frame. At on-resonance condition, this component is exclusively due to the presence of local fields as projected on that axis.

PACS: 61.30.Gd; 76.60.−k

Keywords: Relaxometry; Rotating frame; Local field

1. Introduction

The Larmor frequency dependence of spin-lattice relaxation can be probed in the laboratory frame with the aid of field-cycling nuclear magnetic resonance (NMR) relaxometry [1]. When studying materials with molecular organization, the low-frequency end of the field-cycling relaxation field window may overlap with residual local fields due to non-averaged dipolar or quadrupolar couplings. In addition, eventually non-compensated magnetic fields from the environment may be present. In these cases, the application of a fully adiabatic cycle for the magnetic field becomes a tricky task. While external magnetic fields can be compensated, the presence of local fields (LF) may impose limiting conditions to the applicability of the technique [2,3]. It is therefore desirable to understand all relevant mechanisms that would limit the application of the field-cycling technique. In particular, which would be the lowest Larmor frequency allowing a correct interpretation of the measured dispersion. In addressing this question we found that the problem is essentially related to the nature of local fields. Since, any attempt to investigate this point in the laboratory frame will involve the cycling of the Zeeman magnetic field, we decided to explore the alternative of the rotating frame.

In this paper, we describe a rotating frame technique based on the observation of the detected magnetization intensity after a fixed spin-lock time. The experiment allows to estimate the LF flux density along the laboratory-frame Zeeman-axis. In this context, we define the local field as the sample average of the *residual* (time averaged over molecular dynamics) value of the flux density in the position of a given nuclear spin, due to all the contributions of other spins within the molecule, averaged over all possible spin-positions within the molecule. Since, the model is oriented to mesomorphic phases, intermolecular contributions may be assumed to be negligible due to molecular diffusion.

* Corresponding author. Fax: +54 351 4334054.
E-mail addresses: pj@famaf.unc.edu.ar (J. Perlo), anoardo@famaf.unc.edu.ar (E. Anoardo).

1090-7807/$ - see front matter © 2006 Elsevier Inc. All rights reserved.
doi:10.1016/j.jmr.2006.05.013

This local field is associated in energy terms with residual couplings of dipolar or quadrupolar nature.

In the Section 3, we describe details of the experiment. Then, using a liquid sample with negligible local field, we show that the technique can be used to determine the z component (along the laboratory-frame Zeeman-axis) of the magnetic flux density in the rotating frame due to a preselected offset in the resonance frequency. Finally, we use a similar approach, but on-resonance, to determine the z component of the LF in a nematic phase. In order to observe the temperature dependence of this value, the experiment is considered at three different temperatures.

2. Theory

We define B_{Lz} as the LF component along the laboratory-frame Zeeman-axis. For a nematic specimen, the in-plane (x,y) component of the LF is assumed to be weak due to fast molecular translational diffusion and rotations. For the sake of clarity, in this section we provide a general definition of LF.

The magnetic field generated by a magnetic moment $\mathbf{m}$ is given by [4]

$$\mathbf{B}(\mathbf{r}) = \frac{3\mathbf{n}(\mathbf{n}\cdot\mathbf{m}) - \mathbf{m}}{r^3}, \tag{1}$$

where $\mathbf{n}$ is a unit vector pointing along the position vector $\mathbf{r}$. If the moment $\mathbf{m}$ is due to a spin I oriented along the z-axis:

$$\mathbf{B}(\mathbf{r}) = \frac{3\gamma\hbar I\cos\vartheta\sin\vartheta\cos\varphi}{r^3}\mathbf{i} + \frac{3\gamma\hbar I\cos\vartheta\sin\vartheta\sin\varphi}{r^3}\mathbf{j} + \frac{\gamma\hbar I(3\cos\vartheta^2-1)}{r^3}\mathbf{k}, \tag{2}$$

where r, ϑ, and φ are the spherical coordinates of $\mathbf{r}$.

The projection of this field onto the z-axis is precisely the z-component of the field (2)

$$B_z(\mathbf{r}) = \frac{\gamma\hbar I(3\cos\vartheta^2-1)}{r^3}. \tag{3}$$

The 5CB molecule (4-pentyl-4′-cyanobiphenyl) is constituted by 37 atoms (Fig. 1): 19 protons, 18 carbons, and a nitrogen. Therefore, the magnetic field sensed by a proton will be the sum of contributions of the 18 remaining protons, the 18 carbons, and of the nitrogen. Contributions from nuclei pertaining to other molecules are neglected due to the strong molecular mobility. Then, considering that the protons and the carbons have $I = 1/2$ and the nitrogen has $I = 1$, the field sensed by a proton at the position $\mathbf{r}_j$ belonging to the molecule m is

$$B_z^m(\mathbf{r}_j) = \frac{\hbar}{2}\left[\sum_{p\neq j}^{18}\gamma_P\left\langle\frac{3\cos(\vartheta_{pj}^m)^2-1}{r_{pj}^3}\right\rangle + \sum_{c=1}^{18}\gamma_C\left\langle\frac{3\cos(\vartheta_{cj}^m)^2-1}{r_{cj}^3}\right\rangle + 2\gamma_N\left\langle\frac{3\cos(\vartheta_{nj}^m)^2-1}{r_{nj}^3}\right\rangle\right], \tag{4}$$

where the bracket denotes averaging over time within the time scale imposed by the experiment (*ms*). Since, we are dealing with a low resolution experiment, the mean LF we measure in the experiment is the average of dipolar fields sensed by all the different protons in the sample. Within the molecule m

$$B_z^m = \frac{1}{19}\sum_{j=1}^{19}B_z^m(\mathbf{r}_j). \tag{5}$$

Averaging over the different N molecules:

$$B_{\mathrm{Lz}} = \frac{1}{N}\sum_{m=1}^{N}B_z^m.$$

Different possible molecular orientations are described by an angle Φ, that is, the angle between molecular and Zeeman frames [5]. To generalize, the sum may be replaced by an integration, properly weighed by a function containing the orientational information (i.e., a function of Φ). In this way, we include the information that the mesophase may present a multidomain character. So the LF may be expressed as

$$B_{\mathrm{Lz}} = \frac{1}{19N}\sum_{j=1}^{19}\int B_j(\Phi)P(\Phi)\,\mathrm{d}\Phi, \tag{6}$$

where $B_j(\Phi) = B(\mathbf{r}_j(\Phi))$ is the field for a proton (j) located in a molecule which has a probability $P(\Phi)$ of being oriented with an angle Φ with respect to Zeeman field

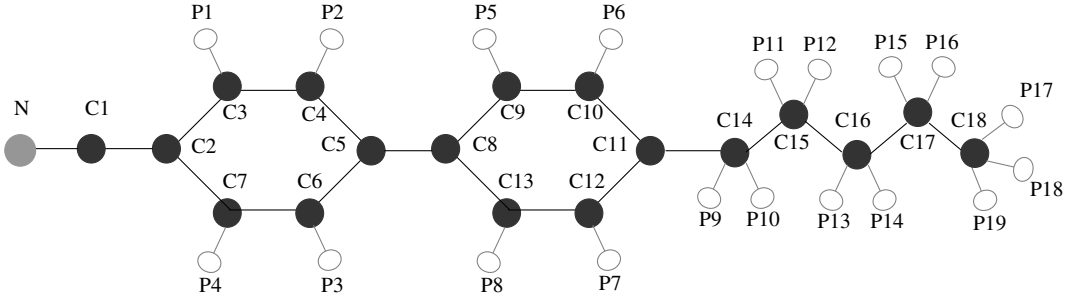

Fig. 1. Schematic diagram of the 5CB molecule. Different atoms are enumerated.

$$B_j(\Phi) = \frac{\hbar}{2}\left[\sum_{p\neq j}^{18}\gamma_P\frac{\eta_{pj}(\Phi)}{\langle r_{pj}^3\rangle} + \sum_{c=1}^{18}\gamma_C\frac{\eta_{cj}(\Phi)}{\langle r_{cj}^3\rangle} + 2\gamma_N\frac{\eta_{nj}(\Phi)}{\langle r_{nj}^3\rangle}\right], \tag{7}$$

where $\eta_{ij}(\Phi) = \langle 3\cos(\vartheta_{ij}^m)^2 - 1\rangle$ with $i = p, c, n$. Finally

$$\begin{aligned} B_{\mathrm{Lz}} = &\frac{1}{38N}\sum_{j=1}^{19}\left[\gamma_P\sum_{p\neq j}^{18}\frac{1}{\langle r_{pj}^3\rangle}\int\eta_{pj}(\Phi)P(\Phi)\,\mathrm{d}\Phi\right] \\ &+\frac{1}{38N}\sum_{j=1}^{19}\left[\gamma_C\sum_{c=1}^{18}\frac{1}{\langle r_{cj}^3\rangle}\int\eta_{cj}(\Phi)P(\Phi)\,\mathrm{d}\Phi\right. \\ &\left.+\frac{2\gamma_N}{\langle r_{nj}^3\rangle}\int\eta_{nj}(\Phi)P(\Phi)\,\mathrm{d}\Phi\right]. \end{aligned} \tag{8}$$

The temperature dependence of the LF is contained within the functions $\eta_{ij}(\Phi)$, $\langle r_{ij}\rangle$ and the probability $P(\Phi)$. This last is strongly dependent on the molecular order (mesophase). The LF is, in a certain extent, an indicative parameter of the level of order of the molecular system at a given temperature. The molecular motion in the isotropic phase has a stochastic character, and no preferential orientational order is present (unless pre-transitional effects are considered). As a consequence, there are no preferred values for Φ, and the probability $P(\Phi)$ that a molecule is being oriented with an angle Φ respect to the Zeeman axis is zero. Therefore, there is not contribution to the local field. Unlike this case, in the nematic phase the molecules are, on average, aligned with their long axes parallel to each other. The mean orientational field is macroscopically described by the mesophase director, showing rotational symmetry. This implies that there is a probability $P(\Phi)$ different from zero in the neighbors of that direction. Within the mesophase, the internal molecular dynamics (group rotations, flexional oscillations of the alkyl-chains, conformational jumps, etc.) is temperature dependent. Such changes are reflected through $\eta_{ij}(\Phi)$ and $\langle r_{ij}\rangle$, which would tend to be smaller at higher temperatures.

3. Experimental technique

The experiment consists in measuring the free induction decay (FID) intensity after a given spin-lock time [6], at different lock radio frequency (RF) field B_1 amplitudes (see Fig. 2A). Due to the fact that nematic compounds in the bulk do not show rotating frame spin-lattice relaxation time ($T_{1\rho}$) dispersion at high Zeeman fields [7], any change in the FID amplitude as B_1 is decreased can be attributed to local fields [8].

The idea beyond the experiment is simple and can be easily described in classical terms (four steps):

1. Fig. 2B represents the effect of the local field during the π/2 RF pulse in the rotating frame. For simplicity, we only show here the z component of the local field (B_{Lz}). During the resonant π/2 pulse the amplitude of the RF field $\mathbf{B}_1$ is much larger than the local field. As a consequence, the effective field $\mathbf{B}_{\mathrm{eff}}$ is practically equal to $\mathbf{B}_1$, and a time δt after the application of the pulse (duration of the π/2 pulse) the magnetization will be in the (x,y) plane of the rotating frame along the y direction.
2. The amplitude of B_1 is reduced and its phase changed by 90° to lock the magnetization (Fig. 2C). If now B_1 becomes comparable to B_{Lz}, the direction and amplitude of the effective field do not coincide any more with that of B_1. Moreover, as $\mathbf{B}_1$ tends to zero, the effective field approaches the local field.
3. The magnetization originally along the y axis will precess around $\mathbf{B}_{\mathrm{eff}}$. After a time $T_{2\rho}$ (transversal relaxation time in the rotating-frame), only the component of the magnetization along the effective field will survive. In case the local field has a component in the (x,y) plane, the only change respect the previous analysis is that the effective field will not be contained in the (y,z) plane.

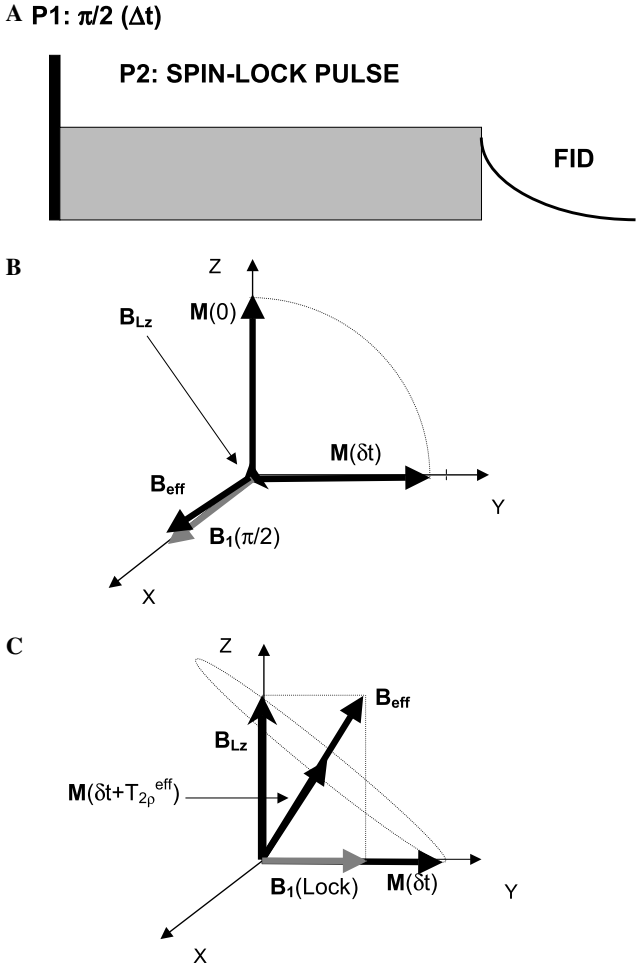

Fig. 2. The fixed lock-time experiment for the measurement of the z-component of the LF. (A) Pulse sequence. (B) Effect of the π/2 pulse of duration δt. During this pulse the B_1 amplitude is much higher than the LF. (C) After a lock-time $T_{2\rho}^{\mathrm{eff}}$, the magnetization will be projected along the effective field.

4. After a spin-lock time of at least $T_{2\rho}$ in a small $\mathbf{B}_1$, the local component of the magnetization becomes reduced in magnitude and pointing along a direction governed by the local field.

If the molecular arrangement has some degree of disorder, the net magnetization will tend to zero as B_1 is decreased to zero. If the sample has a monocrystalline order, the magnetization will also be reduced anyway as B_1 is decreased, unless the local field is uniformly aligned with the y axis. Therefore, the technique also suggest a simple way to check about potential preferential directions of the local fields by a simple repetition of the experiment with a suitable four quadrant phase-cycling scheme.

In spite of common aspects, this experiment may be distinguished from the well-known adiabatic demagnetization in the rotating frame (ADRF) [9], which uses modulation of the Zeeman field or sweeping of the Larmor frequency.

3.1. First case: determination of the offset frequency in the rotating frame: complete motional narrowed LF

As a test experiment, we confronted the well-known value of a preset offset frequency with the corresponding determination obtained from the resulting FID intensity dispersion. A water sample was used for this purpose. It was slightly doped with copper sulphate (less than 0.1%) in order to adjust its spin-lattice relaxation time (T_1).

Case on-resonance. If we irradiate on-resonance, the FID of an isotropic liquid sample after a fixed lock time does not present a dependence with $\mathbf{B}_1$. Since, we are dealing with a liquid sample, we may stick to the weak-collision limit [10]. The spin-lattice relaxation rate in the rotating frame can be written like [8]:

$$\frac{1}{T_{1\rho}} = \frac{K}{4}[J_0(2\omega_1) + \alpha], \tag{9}$$

where $K = (3/2)\gamma^4\hbar^2 I(I+1)$ and $\omega_1 = \gamma B_1$, being $I = 1/2$, γ the giromagnetic ratio of the nuclei and α a constant depending on the molecular motions that are effective for the involved spectral densities that are sensitive to the Larmor frequency ω_0. There is no $T_{1\rho}^{-1}$ dispersion provided the coefficients of the spectral densities and the spectral density J_0 do not depend on the frequency $\nu_1 = \gamma B_1$ (nutation frequency). Thus, being $J_0(2\omega_1)$ constant, $1/T_{1\rho}$ should not be dispersive for a liquid sample at the on-resonance condition.

On these grounds, the FID intensity I_S (proportional to the projected magnetization into the (x,y) plane) should not depend on the value of ν_1 at fixed lock time. However, as can be observed in Fig. 3, there is a slight dispersive slope showing a tendency to lower values of I_S as B_1 increases. This effect was observed at 20 MHz Larmor frequency as well as 300 MHz. It does not depend on the sample nor on the temperature. In the present work, radiation damping effects were measured to be irrelevant. It was verified that this decay responds to the functional form of a cosine, inviting to suppose that an effective rotary saturation takes place during the lock. This latter point will spur more experimental and theoretical effort. Nevertheless, within the context of the current matter, this apparent pitfall lacks relevance. The ν_1 frequency range of interest here is exactly the opposed one, that is, where ν_1 values are less than 40 kHz. In any case, a baseline correction due to this effect was introduced in all data fitting.

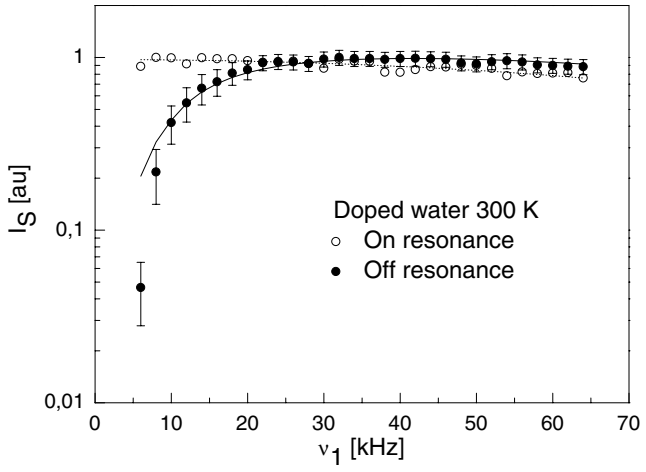

Fig. 3. Signal intensity as a function of the Larmor frequency in the rotating frame ν_1 (fixed lock-time dispersions). Dispersions corresponds to a water sample with adjusted T_1. Open circles correspond to the on-resonance case. Filled circles correspond to an off-resonance preset value of 10 kHz.

Case off-resonance. In this case $I_S(\nu_1)$ presents a noticeable dispersion within the lowest end of the frequency range (see Fig. 3). Now we have two new ingredients:

- The magnetization is locked at the effective field, outside the (x,y) plane.
- Since we are off-resonance, the spectral density coefficients become frequency dependent.

The model needed to determine the offset frequency should therefore be based on these two facts. In the following we analyze the influence of each one on the observed FID after the lock.

3.1.1. $T_{2\rho}^{eff}$ process. Projection of the magnetization into the sensitive (x,y) plane

The effective field $\mathbf{B}_{\text{eff}}$ in the rotating frame can be defined as

$$\mathbf{B}_{\text{eff}} = b_0\mathbf{k} + B_1\mathbf{i}, \tag{10}$$

where $b_0 = B_0 - \omega_{\text{RF}}/\gamma$ represents the off-resonance magnetic field, $B_0 = \omega_0/\gamma$ is the external magnetic flux density defining the Larmor frequency and ω_{RF} is the frequency of the RF field B_1. Thus, the corresponding off-resonance frequency can be expressed as

$$\nu_{\text{off}} = \frac{\gamma B_0 - \omega_{\text{RF}}}{2\pi}. \tag{11}$$

After the $\pi/2$ pulse, the $\mathbf{B}_1$ field intensity is reduced and its phase changed in 90°. Within this picture, due to the presence of the off-resonance component, the magnetization and the lock field in the rotating frame will not be parallel. Moreover, the magnetization will precess in a cone around $\mathbf{B}_{\text{eff}}$. After a time $T_{2\rho}^{\text{eff}}$, the remnant magnetization becomes aligned with $\mathbf{B}_{\text{eff}}$, being its effective value $M_0\cos\theta$, where θ is defined as $\arctan(\frac{b_0}{B_1})$ and M_0 represents the initial equilibrium Curie magnetization with the Zeeman external magnetic field.

In analogy with T_2 and $T_{2\rho}$, the time $T_{2\rho}^{\text{eff}}$ is associated with the loss of coherence of the spins precessing around $\mathbf{B}_{\text{eff}}$. So after $T_{2\rho}^{\text{eff}}$, the remaining magnetization is just the projection of M_0 along $\mathbf{B}_{\text{eff}}$. A second projection should be considered due to the fact that the detection is associated with the sensitive (x, y) plane. Then, the detected intensity is $M_0\cos^2\theta$. This implies that

$$M(\nu_1) \propto \cos^2\left[\arctan\left(\frac{\nu_{\text{off}}}{\nu_1}\right)\right]. \tag{12}$$

3.1.2. Effective spin-lattice relaxation in the rotating frame. ν_1 dispersion

During a spin-lock experiment the magnetization evolves according to the Bloch equations in the rotating frame [11]. The solution of these equations gives [12]

$$M(\tau) = (M_0 - M_{0e})\exp(-\tau/T_{1\rho}^{\text{eff}}) + M_{0e}, \tag{13}$$

where $M(\tau)$ is the magnetization along $\mathbf{B}_{\text{eff}}$, M_0 is the initial spin-locked magnetization, τ is the lock time and $T_{1\rho}^{\text{eff}}$ is the spin-lattice relaxation time in the rotating frame at off-resonance conditions and M_{0e} is the off-resonance equilibrium magnetization that is given by [12]

$$M_{0e} = M_0\frac{T_{1\rho}^{\text{eff}}}{T_1}\cos(\phi), \tag{14}$$

where $\phi = 90 - \theta$ and $\theta = \arctan(\frac{\nu_{\text{off}}}{\nu_1})$.

At on-resonance condition, $T_{1\rho}^{\text{eff}}$ matches $T_{1\rho}$. However, at off resonance condition, the spectral densities coefficients are frequency (ν_1) dependent [14]. Consequently, $T_{1\rho}^{\text{eff}}$ depends on ν_1, still in the case that J_0 does not [13]. The presence of spin-lattice relaxation during the lock time results in a loss of magnetization of dispersive character:

$$\begin{aligned}\frac{1}{T_{1\rho}^{\text{eff}}} &= \frac{1}{T_1}\left[1 + \frac{3\sin^2(\phi)}{2}\right] - \frac{K\sin^2(\phi)}{4}(9J_2 - J_0)\\ &= \frac{1}{T_1} + \left(\frac{3}{2T_1} - d\right)\sin^2(\phi)\\ &= \frac{1}{T_1} + \left(\frac{3}{2T_1} - d\right)\cos^2(\theta),\end{aligned} \tag{15}$$

where $d = K/4(9J_2 - J_0)$ with K constant and J_2, J_0 spectral densities. Then, the magnetization in the rotating frame for a given lock-time τ and off-resonance angle θ is given by:

$$\begin{aligned}M(\nu_1) &= M_0\left[1 - \frac{T_{1\rho}^{\text{eff}}\cos(\phi)}{T_1}\right]\exp(\tau/T_{1\rho}^{\text{eff}}) + M_0\frac{T_{1\rho}^{\text{eff}}\cos(\phi)}{T_1}\\ &= M_0\left[1 - \frac{\sin(\theta)}{1 + (3/2 - T_1 d)\cos^2(\theta)}\right]\\ &\quad\times\exp\left[-\tau\left(\frac{3}{2T_1} - d\right)\cos^2(\theta)\right]\\ &\quad + M_0\frac{\sin(\theta)}{1 + (3/2 - T_1 d)\cos^2(\theta)}.\end{aligned} \tag{16}$$

Finally, from Eqs. (12), (16) and taking into account the cosine base-line correction we get:

$$\begin{aligned}M(\theta(\nu_1)) &= A\cos(c\nu_1)\cos^2(\theta)\frac{\sin(\theta)}{1 + (3/2 - T_1 d)\cos^2(\theta)}\\ &\quad + A\cos(c\nu_1)\cos^2(\theta)\exp\left[-\tau\left(\frac{3}{2T_1} - d\right)\cos^2(\theta)\right]\\ &\quad\times\left[1 - \frac{\sin(\theta)}{1 + (3/2 - T_1 d)\cos^2(\theta)}\right].\end{aligned} \tag{17}$$

This equation will be later used to extract the value of the off-resonance component from data fitting.

3.2. Second case: determination of the local field in the nematic phase

Now, we work at resonance condition. However, the presence of the LF manifests as a non-zero local component along the z axis of the rotating frame. From this point of view, the problem is similar to the previous case: a liquid subjected to an off-resonance spin-lock. However, important differences should be considered:

- The magnetization will still be locked outside the sensitive plane. However, in this case it is due to the presence of the LF.
- As in the former case, a magnetization loss exists due to spin-lattice relaxation. However, in this case the weak collision limit is in conflict with locking conditions at low B_1.
- We have now two distinguishable reservoirs: Zeeman and dipolar. At low values of B_1, these two reservoirs will be strongly coupled thus enabling a new relaxation channel: cross relaxation.

In the following we analyze each in detail.

3.2.1. Locking in the presence of LF

Due to the presence of local field, after a time $T_{2\rho}$ the equilibrium magnetization will be [10]

$$M_{\text{eq}} = \frac{M_0\cos(\theta)}{1 + \left(\frac{B_{\text{Lz}}}{B_{\text{eff}}}\right)^2}. \tag{18}$$

If the lock is produced on-resonance, we have

$$M_{\mathrm{eq}} = \frac{M_0}{1 + (\frac{B_{\mathrm{Lz}}}{B_1})^2}, \tag{19}$$

where B_{Lz} represents the LF component along the Zeeman axis. We note here that if the on-resonance locking field B_1 is large enough, the magnetization loss after a time $T_{2\rho}$ is negligible. However, as B_1 is decreased, an increasing loss of magnetization takes place due to the presence of the LF.

3.2.2. Loss of magnetization by relaxation

The possibility of strong energy exchange between the Zeeman and LF (dipolar) reservoirs does not allow a direct application of the weak collision theory. In this context, we propose to adapt Ailion's approach for solids in the strong collision limit [9]. The two basic assumptions required by the model are:

- The spin temperatures of Zeeman and dipolar systems are equal; i.e., a cross relaxation time between both systems T_{CR} exists so that $T_{\mathrm{CR}} \leqslant \tau_{\mathrm{c}}$, being τ_{c} the correlation time that characterizes the molecular reorientations.
- $\tau_{\mathrm{c}} \ll \omega_0^{-1}$. That is, before and after a molecular jump, the spin orientation is preserved. Consequently, the dipolar energy changes in a sudden form.

Under these suppositions, the spin-lattice relaxation time in the rotating frame becomes:

$$\frac{1}{T_{1\rho}^{\mathrm{eff}}} = \frac{1}{b_0^2 + B_1^2 + B_{\mathrm{Lz}}^2}\left[\frac{b_0^2}{T_a} + \frac{B_1^2}{T_b} + \frac{B_{\mathrm{Lz}}^2}{T_D}\right], \tag{20}$$

where T_a, T_b, and T_D are longitudinal, transversal and dipolar total relaxation times, respectively. T_D includes both contributions due to sudden molecular reorientations, and other contributions or mechanisms that may contribute. In the above discussion we made the silent assumption that the LF for a nematic mainly contributes along the z-axis, as appears to be true experimentally.

If we are on-resonance $b_0 = 0$, and (20) takes the form

$$\frac{1}{T_{1\rho}} = \frac{1}{B_1^2 + B_{\mathrm{Lz}}^2}\left[\frac{B_1^2}{T_b} + \frac{B_{\mathrm{Lz}}^2}{T_D}\right]. \tag{21}$$

The evolution of the magnetization in the rotating-frame as a function of the spin-lock time (τ), for a given off resonance angle is given by

$$M(\nu_1) = \left[M_{\mathrm{eq}} - M_{\rho 0}^{\mathrm{eff}}\right]\exp(-\tau/T_{1\rho}^{\mathrm{eff}}) + M_{\rho 0}^{\mathrm{eff}}, \tag{22}$$

where $M_{\rho 0}^{\mathrm{eff}}$ is

$$M_{\rho 0}^{\mathrm{eff}} = \frac{M_0 B_{\mathrm{eff}}\left[b_0/T_a + B_{\mathrm{Lz}}^2/(B_0 T_D)\right]}{\frac{b_0^2}{T_a} + \frac{B_1^2}{T_b} + \frac{B_{\mathrm{Lz}}^2}{T_D}}. \tag{23}$$

Assuming $B_0 T_D \gg B_{\mathrm{Lz}}^2$, the term $B_L^2/(B_0 T_D)$ in (23) can be neglected. At the on-resonance condition, $M_{\rho 0}^{\mathrm{eff}}$ can thus be neglected, and (22) becomes

$$M(\nu_1) = M_{\mathrm{eq}}\exp(-\tau/T_{1\rho}), \tag{24}$$

where M_{eq} is given by (19).

Finally, the evolution of the magnetization for an on-resonance spin-lock in the presence of LF is

$$M(\nu_1) = \frac{M_0}{1 + (\frac{B_{\mathrm{Lz}}}{B_1})^2}\exp(-\tau/T_{1\rho}), \tag{25}$$

where $T_{1\rho}$ is given by the Eq. (21).

3.2.3. Cross relaxation

In the strong collision limit, Zeeman and dipolar systems are strongly coupled thus relaxing as a whole to the lattice. In this case, the cross relaxation time satisfies the condition $T_{\mathrm{CR}} \leqslant \tau_{\mathrm{c}}$. In the practise, we may assume that in the limit where both reservoirs relax together, $T_{\mathrm{CR}} \approx 0$. In this limit, Eq. (21) suggests that the effective relaxation will be weighted by two contributions: Zeeman (represented by T_b) and dipolar (governed by T_D). On the other extreme, when B_1 surpasses several times the local field, the cross relaxation process becomes inefficient and each reservoir will be characterized by an own spin temperature. In this limit, we see from Eq. (21) that $T_{1\rho} = T_b$. Within this scheme, we assume that T_{CR} increases when increasing B_1, and consequently, Eq. (21) must be modified

$$\frac{1}{T_{1\rho}} = \frac{1}{B_1^2 + B_{\mathrm{Lz}}^2}\left[\frac{B_1^2}{T_b} + \frac{B_{\mathrm{Lz}}^2}{T_D^{\mathrm{eff}}}\right], \tag{26}$$

where now

$$T_D^{\mathrm{eff}} = T_{\mathrm{CR}} + T_D \tag{27}$$

is the effective dipolar relaxation time as observed from the Zeeman reservoir. If the cross relaxation is dominant (strong collision), $T_{\mathrm{CR}} \approx 0$ and we recover the previous equation. If the reservoirs are decoupled (large B_1), $T_{\mathrm{CR}} \gg T_D$ and the observed relaxation is of pure Zeeman character.

To fit the described extreme situations, the cross relaxation time must satisfy:

- To be zero in the limit of zero B_1 locking.
- To increase as B_1 increases.

A Gaussian-type dependence is adopted for T_{CR}, as it is suggested in the literature for the case of solids [10]

$$T_{\mathrm{CR}} = T_D\left[\exp\left[\left(\frac{B_1}{B_{\mathrm{Lz}}}\right)^2\right] - 1\right]. \tag{28}$$

Finally,

$$T_D^{\mathrm{eff}} = T_D\exp\left[\left(\frac{B_1}{B_{\mathrm{Lz}}}\right)^2\right]. \tag{29}$$

Replacing T_D by T_D^{eff} in (21) we get

$$M(\nu_1) = \frac{M_0}{1 + (\frac{B_{1z}}{B_1})^2} \exp\left[\frac{-\tau}{B_1^2 + B_{1z}^2}\left[\frac{B_1^2}{T_b} + \frac{B_{1z}^2}{T_D \exp((\frac{B_1}{B_{1z}})^2)}\right]\right]. \tag{30}$$

This last equation describes the dependence of the locked magnetization on the radio-frequency intensity.

4. Experimental

The intensity of the FID signal was measured as a function of the lock field amplitude B_1 at at fixed lock-time τ. In the first case (doped water) the experiment was done at a well-known off-resonance, while in the second case the experiment was made on- resonance. The covered frequency band was from 6 kHz up to 65 kHz. The lock-time was fixed to 5 ms. The $\pi/2$ pulse length was 2 μs. The working Larmor frequency was 19.181 MHz.

The spin-lattice relaxation time T_1 was measured by using the standard $\pi/2 - \pi/2$ saturation recovery pulse sequence.

The apparatus is based on a Stelar Spinmaster console and a Bruker BE10 electromagnet. The probe was adapted to a Kalmus LP-1000 power transmitter. Sample temperature was directly measured in the sample volume within ±1 K with a CHY 503 digital thermometer. It was verified that for a fixed lock-time of 5 ms and a recycle delay of 5 s (time between spin-lock pulses), the B_1 amplitude can be increased up to 70 kHz with a sample temperature increment of less than 1 K. Sample temperature was controlled by air flux and a home-made controller.

Fig. 3 shows data corresponding to the first case: liquid sample. Doped water was prepared to have $T_1 = (26 \pm 1)$ ms. Measurements were performed at an off-resonance of 10 kHz. Data fitting was done with only two free parameters: ν_{off} and $d = K/4(9J_2 - J_0)$ (see Eq. (17)). The constant c corresponds to the cosine base-line correction and was determined from the on-resonance dispersion: $c = 0.01\ \text{kHz}^{-1}$. Since the FID amplitude was normalized, A was fixed to be 1. Table 1 shows the obtained values from data fitting corresponding to a preset offset of 10 kHz.

The experiment was also done for a $T_1 = (168 \pm 8)$ ms doped water. It was verified that the measured offset does not depend on T_1. From the table we see that, within experimental errors, the measured offset is indistinguishable from the preset value.

LF measurements were done in the nematic phase of 5CB. Experiments were performed at three different temperatures: 298 K (Fig. 4A), 302 K (Fig. 4B), and 306 K (Fig. 4C). The fitting function corresponds to Eq. (30). The two free parameters are B_{1z} and T_D. The relaxation time T_b was considered constant and of the order of the relaxation time corresponding to values of B_1 between 40 and 50 kHz. Due to intrinsic problems related to the standard $T_{1\rho}$ experiment, this time was not measured accurately. However, its value is estimated to be between 100 and 200 ms. To overcome this limitation and to test the relevance of this parameter, fittings were done for both cases. As can be seen in Table 2, the impact of T_b in the results is relatively low.

From the table it can be clearly observed that the z-component of the LF tends to increase as the temperature is lowered. In addition, within experimental errors, we see that T_D is sensitive to a temperature change. However this parameter is mainly related to the efficiency of the coupling between Zeeman and dipolar reservoirs, which in turn strongly depends on the B_1 intensity.

Table 1
Determination of the offset field from data fitting using Eq. (17)

Offset (kHz)	ν_{off} (kHz)	d (ms^{-1})
Water $T_1 = (26 \pm 1)$ ms		
10	9.8 ± 0.3	0.135 ± 0.002

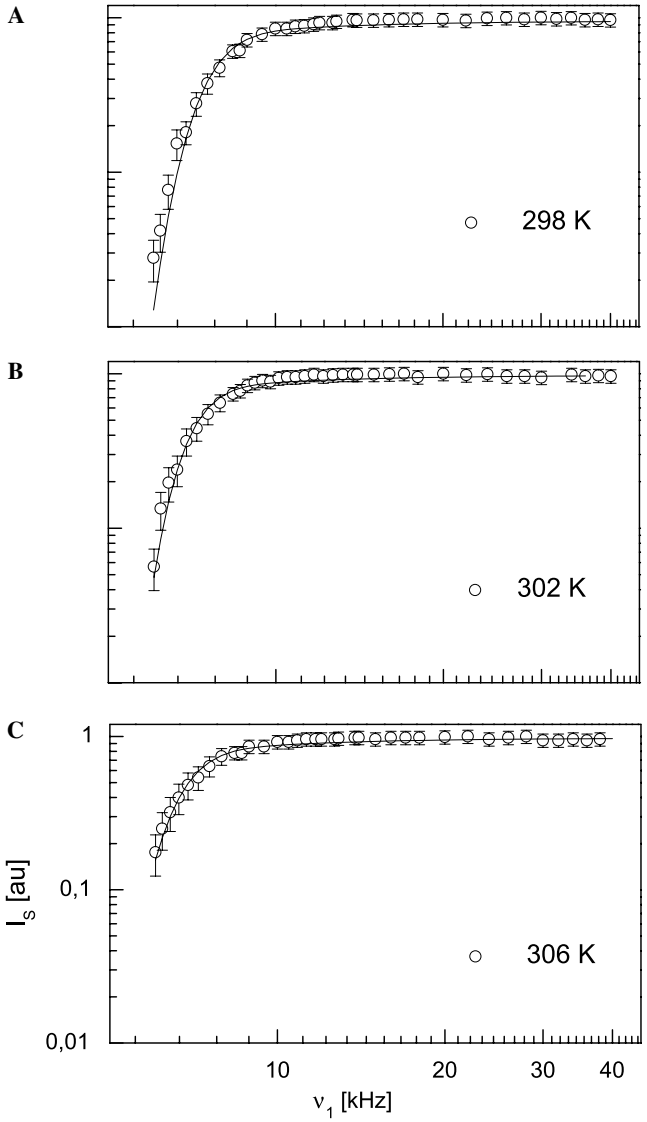

Fig. 4. Fixed lock-time dispersions of the nematic phase of 5CB corresponding to $T_b = 100$ ms. (A) 298 K. (B) 302 K. (C) 306 K.

Table 2
Results for 5CB at different temperatures for two extreme values of T_b

T_b (ms)	B_{Lz} (kHz)	T_D (ms)
5CB $T = (298 \pm 1)$ K		
100	3.8 ± 0.1	0.028 ± 0.009
200	3.94 ± 0.09	0.038 ± 0.009
5CB $T = (302 \pm 1)$ K		
100	3.2 ± 0.1	0.011 ± 0.006
200	3.4 ± 0.1	0.017 ± 0.006
5CB $T = (306 \pm 1)$ K		
100	3.2 ± 0.1	0.021 ± 0.009
200	3.4 ± 0.1	0.031 ± 0.009

It can be observed that within fitting errors, results are not dependent upon the value of T_b in the range from 100 to 200 ms.

5. Conclusions

We have discussed a fixed-time spin-lock rotating frame relaxometry technique. The present experiment was undertaken in order to investigate basic features of LF at low-resolution NMR. The z-component of the LF was determined through a simple theoretical approach.

Obtained values of LF in 5CB are in fine agreement to values of similar parameters determined by other authors in the same and similar compounds by means of other methods. Heteronuclear multiple quantum (HMQ) NMR and local field spectroscopy were used to investigate carbon–proton interactions in liquid crystal molecules [15]. Average dipolar couplings of this sort in 5CB up to 4656 Hz were measured using static proton detected local field spectroscopy (PDLF). In combination with off-magic angle spinning (OMAS), this value showed a reduction to 3473 Hz [16]. Proton encoded local field spectroscopy (PELF) in combination with OMAS were also used in a similar compound (4-cyanobiphenyl hexanoate) obtaining carbon–proton couplings between 52 Hz (for long range interactions) and 5285 Hz (local interactions) [17]. By using proton and deuteron NMR spectroscopy of partially deuterated 5CB (5CB-d_{15}), proton–proton dipolar couplings up to 3919 Hz were found within the molecular core. In this approach the authors simplify the proton spectrum by replacing some protons by deuterons followed by deuteron decoupling [18]. Values of proton–proton dipolar couplings in 5CB around 4000 Hz were obtained by computational calculations [19]. The aforementioned high field NMR techniques are very sensitive to local interactions, allowing to identify different homonuclear and heteronuclear interacting pairs. In our case, we measure a non-localized averaged value including both homo and all heteronuclear interactions. Our experiment is much like the practical situation we have when dealing with field-cycling NMR at low-fields, specially due to the unavoidable strong coupling between the Zeeman and dipolar systems. That is, with the proposed method, we may have a good approximation of the averaged local field sensed in the laboratory frame, i.e., at field-cycling conditions. However, even when the aim of use of these high field techniques are different from our present approach, results should be consistent.

The existence of cross relaxation in solids was discussed in detail in the decades of 60 and 70 [9,10]. In liquid crystals, it was recently invoked in the context of pulsed spin-lock experiments by other members of our group [20]. In this work we proposed a Gaussian-type dependence for the cross relaxation mechanism, in close analogy with the case of solids.

A key aspect of the present study was the extension of Ailion's model for a nematic phase. In this context, the raised question concerns how far the assumptions of the model are satisfied: Zeeman and dipolar reservoirs strongly coupled and, sudden jumps in the dynamics of the system. There is no doubt that when the value of B_1 becomes comparable or smaller than the LF, both Zeeman and dipolar systems couples. As far as a non-zero LF exists, there is no difference from a solid in this aspect.

As B_1 increases, the cross relaxation becomes less efficient until a point where both reservoirs can be considered decoupled. In that limit, the model predicts that in such a case the value of $T_{1\rho}$ tends to a constant value T_b. Starting from the opposed frequency end of the measured interval, that is, from a B_1 value much greater than the LF, $T_{1\rho}$ may be described by the semiclassical approach in the weak collision limit. As far as B_1 increases over the LF value, both approaches tends to a constant non-dispersive value of $T_{1\rho}$. To deal with this apparent conflict, we amalgamated both approaches by the inclusion of a cross relaxation time that controls the passage from one end to the other.

Another feature of the aforementioned model concerns to the molecular dynamics. Although nematic liquid crystals are characterized by cooperative movements, these are not contributing for the spin-lattice relaxation in the rotating frame [8]. Other stochastic processes like molecular reorientations, group rotations, conformational changes, and diffusively translational jumps occur within a broad time scale defined by the corresponding correlation times. Most of these processes may happen in sudden form, whereas the rank of associated correlation times goes from the ps to tens of ms (al least) time scale. Those jumps associated to longer correlation times will be the main contributors in the strong collision limit. Faster processes also contribute through T_D and T_b [9]. Under strong Zeeman-dipolar coupling condition, the cross relaxation time in our experiment resulted of the order of the 100 μs. Consequently, we may assume the existence of a large spectrum of dynamic processes fitting to the strong collision regime. Within this category, those slow and weakly correlated motions will be dominant. In the other extreme, fast stochastic processes will fit with the weak collision limit. In this case, the contribution of slow motions with large correlation time becomes less effective (as far as jumps in the dipolar energy cannot be communicated to the Zeeman reservoir through the cross relaxation mechanism). In between, we may think in a complex mixture of both approaches (this is possible as far as we consider the

coexistence of fast and slow stochastic processes). Nevertheless, a deep description and a detailed formalism is outside the scope of this paper.

A word of caution should be focused in a possible comparison of the proposed method with the traditional $T_{1\rho}$ experiment. In this last case, the magnetization is acquired for different lock-times at a fixed B_1. One important problem in this approach is that the temperature of the sample cannot be held constant throughout the measurement. In particular, this statement holds valid for standard nematic compounds showing $T_{1\rho}$ values longer than 100 ms. This is mainly due to dielectric heating produced by the RF field at high B_1 amplitudes, and to joule heating of the coil. Sample temperature increases with the lock-time. Since, dielectric heating is strongly dependent on the frequency of the RF field, rotating frame experiments are better done at low Larmor frequencies. The problem becomes serious for values of B_1 over 20 kHz, specially if the value of the $T_{1\rho}$ to be measured is over 100 ms. Although the duty cycle is reduced, the problem is also present in pulsed spin-lock experiments. From this point of view, the salient characteristics of the proposed method relays in the fixed lock-time. This can be adjusted according to the maximum B_1 to be scanned while avoiding a relevant sample heating.

Finally, we would like to stress that we found a strong correlation between the obtained values and the corresponding Larmor frequencies at which the field-cycling relaxation dispersion becomes sensitive to local fields. The subject is still under active study. A detailed analysis will be presented elsewhere.

Acknowledgments

We thank economic support from CONICET, Fundación Antorchas and Secyt-UNC. The authors are indebted to G. Ferrante (Stelar srl, Italy) and R. Kimmich (Uni-Ulm, Germany) for the kind donation of instrumental used in this work. E.A. thanks to Alexander von Humboldt Foundation for the support provided through the follow-up programme.

References

[1] R. Kimmich, E. Anoardo, Field-cycling NMR relaxometry, Prog. Nucl. Magn. Reson. Spectrosc. 44 (2004) 257–320.
[2] E. Anoardo, G.M. Ferrante, Magnetic field compensation for field-cycling NMR relaxometry in the ULF band, Appl. Magn. Reson. 24 (2003) 85–96.
[3] E. Anoardo, F. Bonetto, R. Kimmich, Apparent low-field spin-lattice dispersion in the smectic-A mesophase of thermotropic cyanobiphenyls, Phys. Rev. E 68 (022701) (2003) 1–4.
[4] J.D. Jackson, Classical Electrodynamics, Clarendon Press, Oxford, 1962.
[5] B. Stevensson, D. Sandström, A. Maliniak, Conformational distribution functions extracted from residual dipolar couplings: a hybrid model based on maximum entropy and molecular field theory, J. Chem. Phys. 119 (2003) 2738–2746.
[6] E. Fukushima, S.B.W. Roeder, Experimental Pulse NMR: A Nuts and Bolts Approach, Addison-Wesley, Massachusetts, 1981.
[7] M. Vilfan, V. Rutar, S. Žumer, G. Lahajnar, R. Blinc, J.W. Doane, A. Golemme, Proton spin-lattice relaxation in nematic microdroplets, J. Chem. Phys. 89 (1988) 597–604.
[8] E. Anoardo, F. Grinberg, M. Vilfan, R. Kimmich, Proton spin-lattice relaxation in a liquid crystal-Aerosil complex above the bulk isotropization temperature, Chem. Phys. 297 (2004) 99–110.
[9] D.C. Ailion, NMR and ultraslow motions, Adv. Magn. Reson. 5 (1971) 177–227.
[10] A. Abragam, The Principles of Nuclear Magnetism, Clarendon Press, Oxford, 1961.
[11] F. Bloch, Nuclear induction, Phys. Rev. 70 (1946) 460–474.
[12] R. Kimmich, NMR Tomography Diffusometry Relaxometry, Springer-Verlag, Berlin, 1997.
[13] E. Anoardo, C. Hauser, R. Kimmich, Low-frequency molecular dynamics studied by spin-lock field cycling imaging, J. Magn. Reson. 142 (2000) 372–378.
[14] G.P. Jones, Spin-lattice relaxation in the rotating frame: weak-collision case, Phys. Rev. 148 (1966) 332–335.
[15] D.P. Weitekamp, J.R. Garbow, A. Pines, Determination of dipole coupling constants using heteronuclear multiple quantum NMR, J. Chem. Phys. 77 (1982) 2870–2883.
[16] S. Caldarelli, M. Hong, L. Emsley, A. Pines, Measurement of carbon-proton dipolar couplings in liquid crystals by local dipolar field NMR spectroscopy, J. Phys. Chem. 100 (1996) 18696–18701.
[17] C. Canlet, B.M. Fung, Determination of long-range dipolar couplings using mono-deuterated liquid crystals, J. Phys. Chem. B 104 (2000) 6181–6185.
[18] E. Ciampi, G. De Luca, J.W. Emsley, Measurement of interproton, nuclear spin dipolar couplings in liquid crystalline samples by combining variable angle sample spinning, isotope dilution, and deuterium decoupling, J. Magn. Reson. 129 (1997) 207–211.
[19] B. Stevensson, A.V. Komolkin, D. Sanstrm, A. Maliniak, Structure and molecular ordering extracted from residual dipolar couplings: a molecular dynamics simulation study, J. Chem. Phys. 114 (2001) 2332–2339.
[20] R.H. Acosta, R.C. Zamar, G.A. Monti, NMR proton spin dynamics in thermotropic liquid crystals subject to multipulse excitation, Phys. Rev. E 68 (041705) (2003) 1–7.